PARTICLES AND FIELDS • OPEN ACCESS

Luminosity measurements for the *R* scan experiment at BESIII*

Luminosity measurements for the R scan experiment at BESIII *

M. Ablikim(麦迪娜)[1] M. N. Achasov[9,e] S. Ahmed[14] X. C. Ai(艾小聪)[1] O. Albayrak[5] M. Albrecht[4] D. J. Ambrose[44] A. Amoroso[49A,49C] F. F. An(安芬芬)[1] Q. An(安琪)[46,a] J. Z. Bai(白景芝)[1] O. Bakina[23] R. Baldini Ferroli[20A] Y. Ban(班勇)[31] D. W. Bennett[19] J. V. Bennett[5] N. Berger[22] M. Bertani[20A] D. Bettoni[21A] J. M. Bian(边渐鸣)[43] F. Bianchi[49A,49C] E. Boger[23,c] I. Boyko[23] R. A. Briere[5] H. Cai(蔡浩)[51] X. Cai(蔡啸)[1,a] O. Cakir[40A] A. Calcaterra[20A] G. F. Cao(曹国富)[1] S. A. Cetin[40B] J. Chai[49C] J. F. Chang(常劲帆)[1,a] G. Chelkov[23,c,d] G. Chen(陈刚)[1] H. S. Chen(陈和生)[1] J. C. Chen(陈江川)[1] M. L. Chen(陈玛丽)[1,a] S. Chen(陈实)[41] S. J. Chen(陈申见)[29] X. Chen(谌炫)[1,a] X. R. Chen(陈旭荣)[26] Y. B. Chen(陈元柏)[1,a] X. K. Chu(褚新坤)[31] G. Cibinetto[21A] H. L. Dai(代洪亮)[1,a] J. P. Dai(代建平)[34,j] A. Dbeyssi[14] D. Dedovich[23] Z. Y. Deng(邓子艳)[1] A. Denig[22] I. Denysenko[23] M. Destefanis[49A,49C] F. De Mori[49A,49C] Y. Ding(丁勇)[27] C. Dong(董超)[30] J. Dong(董静)[1,a] L. Y. Dong(董燎原)[1] M. Y. Dong(董明义)[1,a] Z. L. Dou(豆正磊)[29] S. X. Du(杜书先)[53] P. F. Duan(段鹏飞)[1] J. Z. Fan(范荆州)[39] J. Fang(方建)[1,a] S. S. Fang(房双世)[1] X. Fang(方馨)[46,a] Y. Fang(方易)[1] R. Farinelli[21A,21B] L. Fava[49B,49C] F. Feldbauer[22] G. Felici[20A] C. Q. Feng(封常青)[46,a] E. Fioravanti[21A] M. Fritsch[14,22] C. D. Fu(傅成栋)[1] Q. Gao(高清)[1] X. L. Gao(高鑫磊)[46,a] Y. Gao(高原宁)[39] Z. Gao(高榛)[46,a] I. Garzia[21A] K. Goetzen[10] L. Gong(龚丽)[30] W. X. Gong(龚文煊)[1,a] W. Gradl[22] M. Greco[49A,49C] M. H. Gu(顾明皓)[1,a] Y. T. Gu(顾运厅)[12] Y. H. Guan(管颖慧)[1] A. Q. Guo(郭爱强)[1] L. B. Guo(郭立波)[28] R. P. Guo(郭如盼)[1] Y. Guo(郭月)[1] Y. P. Guo(郭玉萍)[22] Z. Haddadi[25] A. Hafner[22] S. Han(韩爽)[51] X. Q. Hao(郝喜庆)[15] F. A. Harris[42] K. L. He(何康林)[1] F. H. Heinsius[4] T. Held[4] Y. K. Heng(衡月昆)[1,a] T. Holtmann[4] Z. L. Hou(侯治龙)[1] C. Hu(胡琛)[28] H. M. Hu(胡海明)[1] J. F. Hu(胡继峰)[49A,49C] T. Hu(胡涛)[1,a] Y. Hu(胡誉)[1] G. S. Huang(黄光顺)[46,a] J. S. Huang(黄金书)[15] X. T. Huang(黄性涛)[33] X. Z. Huang(黄晓忠)[29] Z. L. Huang(黄智玲)[27] T. Hussain[48] W. Ikegami Andersson[50] Q. Ji(纪全)[1] Q. P. Ji(姬清平)[15] X. B. Ji(季晓斌)[1] X. L. Ji(季筱璐)[1,a] L. W. Jiang(姜鲁文)[51] X. S. Jiang(江晓山)[1,a] X. Y. Jiang(蒋兴雨)[30] J. B. Jiao(焦健斌)[33] Z. Jiao(焦铮)[17] D. P. Jin(金大鹏)[1,a] S. Jin(金山)[1] T. Johansson[50] A. Julin[43] N. Kalantar-Nayestanaki[25] X. L. Kang(康晓琳)[1] X. S. Kang(康晓坤)[30] M. Kavatsyuk[25] B. C. Ke(柯百谦)[5] P. Kiese[22] R. Kliemt[10] B. Kloss[22] O. B. Kolcu[40B,h] B. Kopf[4] M. Kornicer[42] A. Kupsc[50] W. Kühn[24] J. S. Lange[24] M. Lara[19] P. Larin[14] H. Leithoff[22] C. Leng[49C] C. Li(李翠)[50] Cheng Li(李澄)[46,a] D. M. Li(李德民)[53] F. Li(李飞)[1,a] F. Y. Li(李峰云)[31] G. Li(李刚)[1] H. B. Li(李海波)[1] H. J. Li(李惠静)[1] J. C. Li(李家才)[1] Jin Li(李瑾)[32] K. Li(李康)[13] K. Li(李科)[33] Lei Li(李蕾)[3] P. R. Li(李培荣)[7,41] Q. Y. Li(李启云)[33] T. Li(李腾)[33] W. D. Li(李卫东)[1] W. G. Li(李卫国)[1] X. L. Li(李晓玲)[33] X. N. Li(李小男)[1,a] X. Q. Li(李学潜)[30] Y. B. Li(李郁博)[2] Z. B. Li(李志兵)[38] H. Liang(梁昊)[46,a] Y. F. Liang(梁勇飞)[36] Y. T. Liang(梁羽铁)[24] G. R. Liao(廖广睿)[11] D. X. Lin(林德旭)[14] B. Liu(刘冰)[34,j] B. J. Liu(刘北江)[1] C. X. Liu(刘春秀)[1] D. Liu(刘栋)[46,a] F. H. Liu(刘福虎)[35] Fang Liu(刘芳)[1] Feng Liu (刘峰)[6] H. B. Liu(刘宏邦)[12] H. H. Liu(刘汇慧)[16] H. H. Liu(刘欢欢)[1] H. M. Liu(刘怀民)[1] J. Liu(刘杰)[1] J. B. Liu(刘建北)[46,a] J. P. Liu(刘觉平)[51] J. Y. Liu(刘晶译)[1] K. Liu(刘凯)[39] K. Y. Liu(刘魁勇)[27] L. D. Liu(刘兰雕)[31] P. L. Liu(刘佩莲)[1,a] Q. Liu(刘倩)[41] S. B. Liu(刘树彬)[46,a] X. Liu(刘翔)[26] Y. B. Liu(刘玉斌)[30] Y. Y. Liu(刘媛媛)[30] Z. A. Liu(刘振安)[1,a] Zhiqing Liu(刘智青)[22] H. Loehner[25] X. C. Lou(娄辛丑)[1,a,g] H. J. Lu(吕海江)[17] J. G. Lu(吕军光)[1,a] Y. Lu(卢宇)[1] Y. P. Lu(卢云鹏)[1,a] C. L. Luo(罗成林)[28] M. X. Luo(罗民兴)[52] T. Luo[42] X. L. Luo(罗小兰)[1,a] X. R. Lyu(吕晓睿)[41] F. C. Ma(马凤才)[27] H. L. Ma(马海龙)[1] L. L. Ma(马连良)[33] M. M. Ma(马明明)[1] Q. M. Ma(马秋梅)[1] T. Ma(马天)[1] X. N. Ma(马旭宁)[30] X. Y. Ma(马骁妍)[1,a]

Received 8 February 2017

∗ Supported by National Key Basic Research Program of China (2015CB856700), National Natural Science Foundation of China (NSFC) (10935007, 11121092, 11125525, 11235011, 11322544, 11335008, 11375170, 11275189, 11079030, 11475164, 11475169, 11005109, 10979095, 11275211), Chinese Academy of Sciences (CAS) Large-Scale Scientific Facility Program; Joint Large-Scale Scientific Facility Funds of the NSFC and CAS (11179007, U1232201, U1332201, U1532102). (KJCX2-YW-N29, KJCX2-YW-N45). 100 Talents Program of CAS, INPAC and Shanghai Key Laboratory for Particle Physics and Cosmology, German Research Foundation DFG (Collaborative Research Center CRC-1044), Istituto Nazionale di Fisica Nucleare, Italy, Ministry of Development of Turkey (DPT2006K-120470), Russian Foundation for Basic Research (14-07-91152), U. S. Department of Energy (DE-FG02-04ER41291, DE-FG02-05ER41374, DE-FG02-94ER40823, DESC0010118), U.S. National Science Foundation, University of Groningen (RuG) and the Helmholtzzentrum fuer Schwerionenforschung GmbH (GSI), Darmstadt, WCU Program of National Research Foundation of Korea (R32-2008-000-10155-0)

Y. M. Ma(马玉明)[33] F. E. Maas[14] M. Maggiora[49A,49C] Q. A. Malik[48] Y. J. Mao(冒亚军)[31] Z. P. Mao(毛泽普)[1] S. Marcello[49A,49C] J. G. Messchendorp[25] G. Mezzadri[21B] J. Min(闵建)[1,a] T. J. Min(闵天觉)[1] R. E. Mitchell[19] X. H. Mo(莫晓虎)[1,a] Y. J. Mo(莫玉俊)[6] C. Morales Morales[14] N. Yu. Muchnoi[9,e] H. Muramatsu[43] P. Musiol[4] Y. Nefedov[23] F. Nerling[10], I. B. Nikolaev[9,e] Z. Ning(宁哲)[1,a] S. Nisar[8] S. L. Niu(牛顺利)[1,a], X. Y. Niu(牛讯伊)[1] S. L. Olsen(马鹏)[32], Q. Ouyang(欧阳群)[1,a] S. Pacetti[20B], Y. Pan(潘越)[46,a] P. Patteri[20A] M. Pelizaeus[4] H. P. Peng(彭海平)[46,a] K. Peters[10,i] J. Pettersson[50] J. L. Ping(平加伦)[28] R. G. Ping(平荣刚)[1] R. Poling[43] V. Prasad[1] H. R. Qi(漆红荣)[2] M. Qi(祁鸣)[29] S. Qian(钱森)[1,a] C. F. Qiao(乔从丰)[41] L. Q. Qin(秦丽清)[33] N. Qin(覃拈)[51] X. S. Qin(秦小帅)[1] Z. H. Qin(秦中华)[1,a] J. F. Qiu(邱进发)[1] K. H. Rashid[48,k] C. F. Redmer[22] M. Ripka[22] G. Rong(荣刚)[1] Ch. Rosner[14] X. D. Ruan(阮向东)[12] A. Sarantsev[23,f] M. Savrié[21B] C. Schnier[4] K. Schoenning[50] W. Shan(单葳)[31] M. Shao(邵明)[46,a] C. P. Shen(沈成平)[2] P. X. Shen(沈培迅)[30] X. Y. Shen(沈肖雁)[1] H. Y. Sheng(盛华义)[1] W. M. Song(宋维民)[1] X. Y. Song(宋欣颖)[1] S. Sosio[49A,49C] S. Spataro[49A,49C] G. X. Sun(孙功星)[1] J. F. Sun(孙俊峰)[15] S. S. Sun(孙胜森)[1] X. H. Sun(孙新华)[1] Y. J. Sun(孙勇杰)[46,a] Y. Z. Sun(孙永昭)[1] Z. J. Sun(孙志嘉)[1,a] Z. T. Sun(孙振田)[19] C. J. Tang(唐昌建)[36] X. Tang(唐晓)[1] I. Tapan[40C] E. H. Thorndike[44] M. Tiemens[25] I. Uman[40D] G. S. Varner[42] B. Wang(王斌)[30] B. L. Wang(王滨龙)[41] D. Wang(王东)[31] D. Y. Wang(王大勇)[31] K. Wang(王科)[1,a] L. L. Wang(王亮亮)[1] L. S. Wang(王灵淑)[1] M. Wang(王萌)[33] P. Wang(王平)[1] P. L. Wang(王佩良)[1] W. Wang(王炜)[1,a] W. P. Wang(王维平)[46,a] X. F. Wang(王雄飞)[39] Y. Wang(王越)[37] Y. D. Wang(王雅迪)[14] Y. F. Wang(王贻芳)[1,a] Y. Q. Wang(王亚乾)[22] Z. Wang(王铮)[1,a] Z. G. Wang(王志刚)[1,a] Z. H. Wang(王志宏)[46,a] Z. Y. Wang(王至勇)[1] Z. Y. Wang(王宗源)[1] T. Weber[22] D. H. Wei(魏代会)[11] P. Weidenkaff[22] S. P. Wen(文硕频)[1] U. Wiedner[4] M. Wolke[50] L. H. Wu(伍灵慧)[1] L. J. Wu(吴连近)[1] Z. Wu(吴智)[1,a] L. Xia(夏磊)[46,a] L. G. Xia(夏力钢)[39] Y. Xia(夏宇)[18] D. Xiao(肖栋)[1] H. Xiao(肖浩)[47] Z. J. Xiao(肖振军)[28] Y. G. Xie(谢宇广)[1,a] Y. H. Xie(谢跃红)[6] Q. L. Xiu(修青磊)[1,a] G. F. Xu(许国发)[1] J. J. Xu(徐静静)[1] L. Xu(徐雷)[1] Q. J. Xu(徐庆君)[13] Q. N. Xu(徐庆年)[41] X. P. Xu(徐新平)[37] L. Yan(严亮)[49A,49C] W. B. Yan(鄢文标)[46,a] W. C. Yan(闫文成)[46,a] Y. H. Yan(颜永红)[18] H. J. Yang(杨海军)[34,j] H. X. Yang(杨洪勋)[1] L. Yang(杨柳)[51] Y. X. Yang(杨永栩)[11] M. Ye(叶梅)[1,a] M. H. Ye(叶铭汉)[7] J. H. Yin(殷俊昊)[1] Z. Y. You(尤郑昀)[38] B. X. Yu(俞伯祥)[1,a] C. X. Yu(喻纯旭)[30] J. S. Yu(俞洁晟)[26] C. Z. Yuan(苑长征)[1] Y. Yuan(袁野)[1] A. Yuncu[40B,b] A. A. Zafar[48] Y. Zeng(曾云)[18] Z. Zeng(曾哲)[46,a] B. X. Zhang(张丙新)[1] B. Y. Zhang(张炳云)[1,a] C. C. Zhang(张长春)[1] D. H. Zhang(张达华)[1] H. H. Zhang(张宏浩)[38] H. Y. Zhang(章红宇)[1,a] J. Zhang(张晋)[1] J. J. Zhang(张佳佳)[1] J. L. Zhang(张杰磊)[1] J. Q. Zhang(张敬庆)[1] J. W. Zhang(张家文)[1,a] J. Y. Zhang(张建勇)[1] J. Z. Zhang(张景芝)[1] K. Zhang(张坤)[1] L. Zhang(张磊)[1] S. Q. Zhang(张士权)[30] X. Y. Zhang(张学尧)[33] Y. Zhang(张瑶)[1] Y. Zhang(张洋)[1] Y. H. Zhang(张银鸿)[1,a] Y. N. Zhang(张宇宁)[41] Y. T. Zhang(张亚腾)[46,a] Yu Zhang(张宇)[41] Z. H. Zhang(张正好)[6] Z. P. Zhang(张子平)[46] Z. Y. Zhang(张振宇)[51] G. Zhao(赵光)[1] J. W. Zhao(赵京伟)[1,a] J. Y. Zhao(赵静宜)[1] J. Z. Zhao(赵京周)[1,a] Lei Zhao(赵雷)[46,a] Ling Zhao(赵玲)[1] M. G. Zhao(赵明刚)[30] Q. Zhao(赵强)[1] Q. W. Zhao(赵庆旺)[1] S. J. Zhao(赵书俊)[53] T. C. Zhao(赵天池)[1] Y. B. Zhao(赵豫斌)[1,a] Z. G. Zhao(赵政国)[46,a] A. Zhemchugov[23,c] B. Zheng(郑波)[14,47] J. P. Zheng(郑建平)[1,a] W. J. Zheng(郑文静)[33] Y. H. Zheng(郑阳恒)[41] B. Zhong(钟彬)[28] L. Zhou(周莉)[1,a] X. Zhou(周详)[51] X. K. Zhou(周晓康)[46,a] X. R. Zhou(周小蓉)[46,a] X. Y. Zhou(周兴玉)[1] K. Zhu(朱凯)[1] K. J. Zhu(朱科军)[1,a] S. Zhu(朱帅)[1] S. H. Zhu(朱世海)[45] X. L. Zhu(朱相雷)[39] Y. C. Zhu(朱莹春)[46,a] Y. S. Zhu(朱永生)[1] Z. A. Zhu(朱自安)[1] J. Zhuang(庄建)[1,a] L. Zotti[49A,49C] B. S. Zou(邹冰松)[1] J. H. Zou(邹佳恒)[1]

(BESIII Collaboration)

[1] Institute of High Energy Physics, Beijing 100049, China
[2] Beihang University, Beijing 100191, China
[3] Beijing Institute of Petrochemical Technology, Beijing 102617, China
[4] Bochum Ruhr-University, D-44780 Bochum, Germany
[5] Carnegie Mellon University, Pittsburgh, Pennsylvania 15213, USA
[6] Central China Normal University, Wuhan 430079, China
[7] China Center of Advanced Science and Technology, Beijing 100190, China
[8] COMSATS Institute of Information Technology, Lahore, Defence Road, Off Raiwind Road, 54000 Lahore, Pakistan
[9] G.I. Budker Institute of Nuclear Physics SB RAS (BINP), Novosibirsk 630090, Russia
[10] GSI Helmholtzcentre for Heavy Ion Research GmbH, D-64291 Darmstadt, Germany
[11] Guangxi Normal University, Guilin 541004, China
[12] Guangxi University, Nanning 530004, China
[13] Hangzhou Normal University, Hangzhou 310036, China
[14] Helmholtz Institute Mainz, Johann-Joachim-Becher-Weg 45, D-55099 Mainz, Germany
[15] Henan Normal University, Xinxiang 453007, China
[16] Henan University of Science and Technology, Luoyang 471003, China
[17] Huangshan College, Huangshan 245000, China
[18] Hunan University, Changsha 410082, China

[19] Indiana University, Bloomington, Indiana 47405, USA
[20] (A)INFN Laboratori Nazionali di Frascati, I-00044, Frascati, Italy; (B)INFN and University of Perugia, I-06100, Perugia, Italy
[21] (A)INFN Sezione di Ferrara, I-44122, Ferrara, Italy; (B)University of Ferrara, I-44122, Ferrara, Italy
[22] Johannes Gutenberg University of Mainz, Johann-Joachim-Becher-Weg 45, D-55099 Mainz, Germany
[23] Joint Institute for Nuclear Research, 141980 Dubna, Moscow region, Russia
[24] Justus-Liebig-Universitaet Giessen, II. Physikalisches Institut, Heinrich-Buff-Ring 16, D-35392 Giessen, Germany
[25] KVI-CART, University of Groningen, NL-9747 AA Groningen, The Netherlands
[26] Lanzhou University, Lanzhou 730000, China
[27] Liaoning University, Shenyang 110036, China
[28] Nanjing Normal University, Nanjing 210023, China
[29] Nanjing University, Nanjing 210093, China
[30] Nankai University, Tianjin 300071, China
[31] Peking University, Beijing 100871, China
[32] Seoul National University, Seoul, 151-747 Korea
[33] Shandong University, Jinan 250100, China
[34] Shanghai Jiao Tong University, Shanghai 200240, China
[35] Shanxi University, Taiyuan 030006, China
[36] Sichuan University, Chengdu 610064, China
[37] Soochow University, Suzhou 215006, China
[38] Sun Yat-Sen University, Guangzhou 510275, China
[39] Tsinghua University, Beijing 100084, China
[40] (A)Ankara University, 06100 Tandogan, Ankara, Turkey; (B)Istanbul Bilgi University, 34060 Eyup, Istanbul, Turkey; (C)Uludag University, 16059 Bursa, Turkey; (D)Near East University, Nicosia, North Cyprus, Mersin 10, Turkey
[41] University of Chinese Academy of Sciences, Beijing 100049, China
[42] University of Hawaii, Honolulu, Hawaii 96822, USA
[43] University of Minnesota, Minneapolis, Minnesota 55455, USA
[44] University of Rochester, Rochester, New York 14627, USA
[45] University of Science and Technology Liaoning, Anshan 114051, China
[46] University of Science and Technology of China, Hefei 230026, China
[47] University of South China, Hengyang 421001, China
[48] University of the Punjab, Lahore-54590, Pakistan
[49] (A)University of Turin, I-10125, Turin, Italy; (B)University of Eastern Piedmont, I-15121, Alessandria, Italy; (C)INFN, I-10125, Turin, Italy
[50] Uppsala University, Box 516, SE-75120 Uppsala, Sweden
[51] Wuhan University, Wuhan 430072, China
[52] Zhejiang University, Hangzhou 310027, China
[53] Zhengzhou University, Zhengzhou 450001, China

[a] Also at State Key Laboratory of Particle Detection and Electronics, Beijing 100049, Hefei 230026, China
[b] Also at Bogazici University, 34342 Istanbul, Turkey
[c] Also at the Moscow Institute of Physics and Technology, Moscow 141700, Russia
[d] Also at the Functional Electronics Laboratory, Tomsk State University, Tomsk, 634050, Russia
[e] Also at the Novosibirsk State University, Novosibirsk, 630090, Russia
[f] Also at the NRC "Kurchatov Institute", PNPI, 188300, Gatchina, Russia
[g] Also at University of Texas at Dallas, Richardson, Texas 75083, USA
[h] Also at Istanbul Arel University, 34295 Istanbul, Turkey
[i] Also at Goethe University Frankfurt, 60323 Frankfurt am Main, Germany
[j] Also at Key Laboratory for Particle Physics, Astrophysics and Cosmology, Ministry of Education; Shanghai Key Laboratory for Particle Physics and Cosmology; Institute of Nuclear and Particle Physics, Shanghai 200240, China
[k] Government College Women University, Sialkot - 51310. Punjab, Pakistan

Abstract: By analyzing the large-angle Bhabha scattering events $e^+e^- \to (\gamma)e^+e^-$ and diphoton events $e^+e^- \to (\gamma)\gamma\gamma$ for the data sets collected at center-of-mass (c.m.) energies between 2.2324 and 4.5900 GeV (131 energy points in total) with the upgraded Beijing Spectrometer (BESIII) at the Beijing Electron-Positron Collider (BEPCII), the integrated luminosities have been measured at the different c.m. energies, individually. The results are important inputs for the R value and J/ψ resonance parameter measurements.

Keywords: luminosity, Bhabha, diphoton, R value

PACS: 13.66.De, 13.66.Jn **DOI:** 10.1088/1674-1137/41/6/063001

1 Introduction

Hadron production in e^+e^- annihilation is one of the most valuable testing grounds for Quantum Chromodynamics (QCD), and is an important input for precision tests of the Standard Model (SM). The R value, which is defined as the lowest-level hadronic cross section normalized to the theoretical $\mu^+\mu^-$ production cross section in e^+e^- annihilation, is an indispensable input for the determination of the non-perturbative hadronic contribution to the electromagnetic coupling constant evaluated at the Z pole ($\alpha(M_Z^2)$) [1, 2], and the anomalous magnetic moment $a_\mu = (g-2)/2$ of the muon [3]. The dominant uncertainties in both $\alpha(M_Z^2)$ and a_μ measurements are due to the effects of hadronic vacuum polarization, which cannot be reliably calculated in the low energy region. Instead, with the application of dispersion relations, experimentally measured R values can determine the effect of vacuum polarization.

Experimentally, the R value is determined from

$$R=\frac{N_{\rm had}^{\rm obs}-N_{\rm had}^{\rm bkg}}{\sigma_{\mu\mu}^0\cdot\mathcal{L}\cdot\varepsilon_{\rm had}\cdot\varepsilon_{\rm had}^{\rm trig}\cdot(1+\delta)}, \qquad (1)$$

where $N_{\rm had}^{\rm obs}$ is the number of observed hadronic events, $N_{\rm had}^{\rm bkg}$ is the number of background events, $\mathcal{L}$ is the integrated luminosity, $\varepsilon_{\rm had}$ is the detection efficiency for the hadron event selection, $\varepsilon_{\rm had}^{\rm trig}$ is the trigger efficiency, $1+\delta$ is the initial-state radiation (ISR) correction factor, and $\sigma_{\mu\mu}^0$ is the Born cross section of $e^+e^-\to\mu^+\mu^-$. Therefore, the measurement of integrated luminosity plays an important role in the R value measurement.

Quantum electrodynamics (QED) processes are usually applied to determine the integrated luminosity, due to larger production rates, simpler final-state topologies and more accurate cross section calculation in theory relative to the other processes. The integrated luminosity is determined from

$$\mathcal{L}=\frac{N_{\rm QED}^{\rm obs}-N_{\rm QED}^{\rm bkg}}{\sigma_{\rm QED}\cdot\varepsilon_{\rm QED}\cdot\varepsilon_{\rm QED}^{\rm trig}}, \qquad (2)$$

where $N_{\rm QED}^{\rm obs}$ is the number of QED events observed in the experimental data, $N_{\rm QED}^{\rm bkg}$ is the number of background events, $\sigma_{\rm QED}$ is the cross section of the selected QED process, $\varepsilon_{\rm QED}$ is the detection efficiency and $\varepsilon_{\rm QED}^{\rm trig}$ is the trigger efficiency.

In this paper, we present the measurements of luminosities of the R scan data samples taken at BESIII from 2012 to 2014. The measurements are performed by analyzing two QED processes, $e^+e^-\to(\gamma)e^+e^-$ and $e^+e^-\to(\gamma)\gamma\gamma$. For energy points near the J/ψ resonance, only the $e^+e^-\to(\gamma)\gamma\gamma$ process is used, because the Monte Carlo (MC) simulation at the J/ψ resonance is sensitive to the c.m. energy and is imperfect.

2 Detector

BEPCII [4] is a double-ring e^+e^- collider designed to provide a peak luminosity of 10^{33} cm$^{-2}\cdot$s^{-1} at a c.m. energy ($\sqrt{s}$) of 3770 MeV. The BESIII [4] detector has a geometrical acceptance of 93% of 4π and has four main detector sub-components as follows. (1) A small-cell, helium-based (60% He, 40% C_3H_8) main drift chamber (MDC) with 43 layers providing an average single-hit resolution of 135 μm, and charged-particle momentum resolution in a 1 T magnetic field of 0.5% at 1 GeV/c. (2) An electromagnetic calorimeter (EMC) consisting of 6240 CsI(Tl) crystals in a cylindrical structure arranged in a barrel and two endcaps. The energy resolution at 1.0 GeV is 2.5% (5%) in the barrel (endcaps), and the position resolution is 6 mm (9 mm) in the barrel (endcaps). (3) A time-of-flight (TOF) system for particle identification composed of a barrel part made of two layers with 88 pieces of 5 cm thick, 2.4 m long plastic scintillator in each layer, and two endcaps with 96 fan-shaped, 5 cm thick, plastic scintillators in each endcap. The time resolution of 80 ps (110 ps) for the barrel (endcap) provides 2σ K/π separation for momenta up to ~ 1.0 GeV/c. (4) A muon system (MUC) consisting of 1000 m^2 of resistive plate chambers in nine (eight) layers of barrel (endcap) provides 2 cm position resolution.

3 Data sample and Monte Carlo simulation

The measurements of luminosities were performed for 131 data samples, including 4 energy points at 2.2324, 2.4000, 2.8000, 3.4000 GeV taken at the 2012 run, 104 energy points from 3.8500 to 4.5900 GeV taken at the 2013–2014 runs, 15 energy points near the J/ψ production threshold, 4 energy points during the τ mass measurement and 4 energy points for charmonium studies.

The $e^+e^-\to(\gamma)e^+e^-$, $(\gamma)\gamma\gamma$ and $(\gamma)\mu^+\mu^-$ events were simulated with the generator Babayaga v3.5 [5–7]. The background process of $e^+e^-\to\tau^+\tau^-$ was generated with the KKMC [8], while the $e^+e^-\to$ hadrons and $e^+e^-\to e^+e^- + X$ (X can be hadrons or leptons) events were generated with LUARLW [9] and BesTwogam [10], respectively.

4 Analysis

The $e^+e^-\to(\gamma)e^+e^-$ events are required to have two good charged tracks with opposite charge. Each charged track is required to be within ±10 cm of the interaction point in the beam direction and 1 cm in the plane perpendicular to the beam. In addition, the charged tracks are required to be within $|\cos\theta| < 0.8$, where θ is the polar angle, in the MDC. Without applying further particle identification, the tracks are assigned as electron and positron depending on their charges. The deposited energies of electron and positron ($E_{e^\pm}$) in the EMC are required to be larger than $0.65\times E_{\rm beam}$ to suppress backgrounds, where $E_{\rm beam}$ is the beam energy. To make sure the selected charged tracks are back to back in the c.m. system, $|\Delta\theta_{e^\pm}| = |\theta_1+\theta_2-180°| < 10.0°$ and $|\Delta\phi_{e^\pm}| = ||\phi_1-\phi_2|-180°| < 5.0°$ are required, where $\theta_{1/2}$ and $\phi_{1/2}$ are the polar and azimuthal angles of the two charged tracks, respectively. Figure 1 shows comparisons of the momentum and polar angle distributions of electrons and positrons between experimental data and MC simulation at $\sqrt{s} = 2.2324$ GeV. Good agreement is observed.

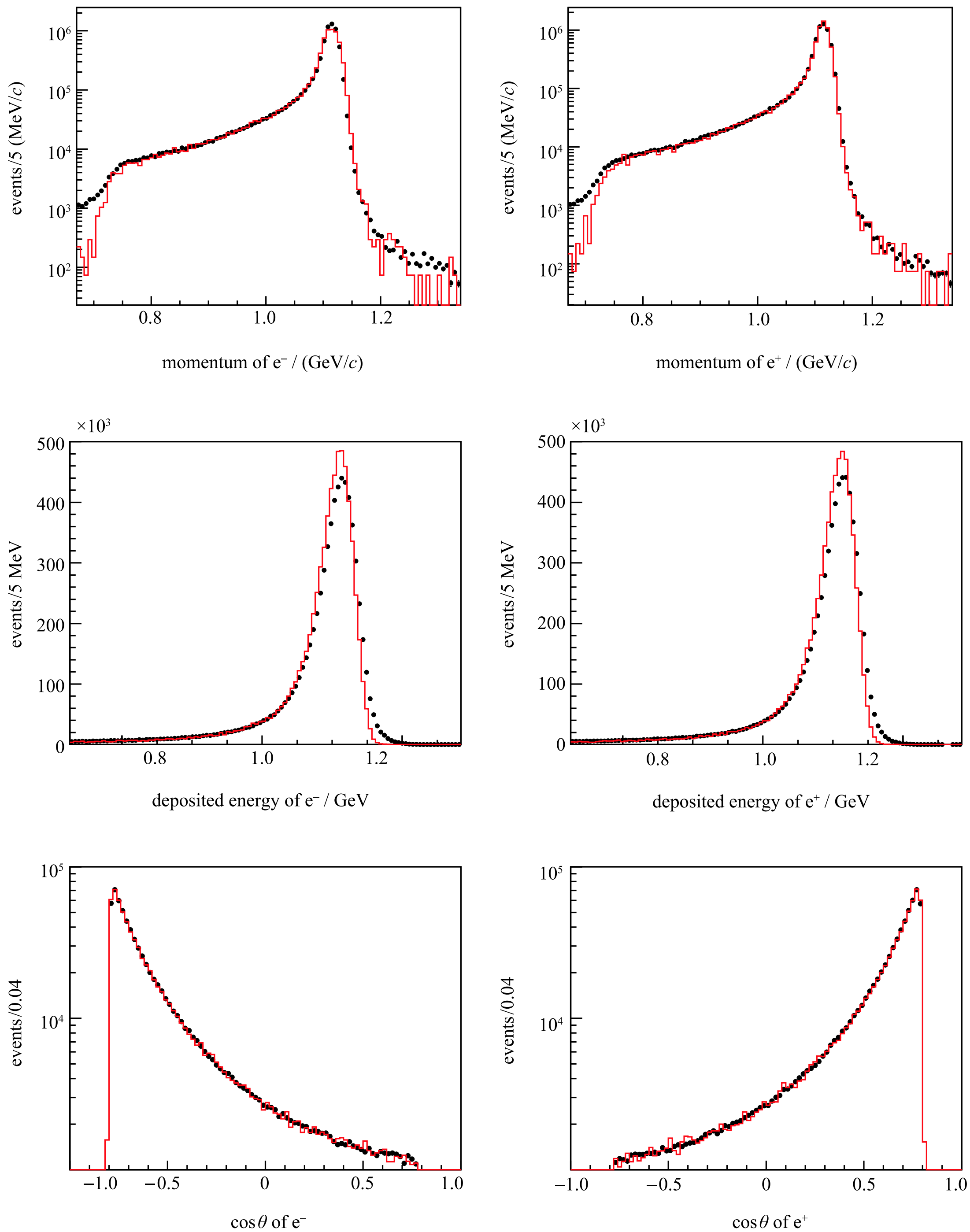

Fig. 1. (color online) The distributions of momentum (upper plots), deposited energy (middle plots) and polar angle $\cos\theta$ (lower plots) for electrons (left) and positrons (right) at $\sqrt{s} = 2.2324$ GeV. Dots with error bars are experimental data and red histograms are signal MC simulation. The MC entries are normalized to the experimental data.

To select $e^+e^- \rightarrow (\gamma)\gamma\gamma$ events, the number of good charged tracks is required to be zero. Two neutral clusters are required to have a polar angle $|\cos\theta| < 0.8$ with the deposited energy E_γ satisfying $0.7 < E_\gamma/E_{\rm beam} < 1.16$. The two selected photon candidates are further required to be back to back by applying the requirement $|\Delta\phi_\gamma| = |\phi_{\gamma1} - \phi_{\gamma2}| < 2.5°$, where $\phi_{\gamma1/2}$ are the azimuthal anlge of the photons. Figure 2 shows comparisons of the energy deposition, polar angle and $\Delta\phi_\gamma$ distributions of two selected photons between experimental data and MC simulation at $\sqrt{s} = 2.2324$ GeV.

The numbers of observed QED events, $N^{\rm obs}_{\rm QED}$, are obtained by event counting after applying the event selection requirements to experimental data at different c.m. energies, individually. The detection efficiencies of signals, $\varepsilon_{\rm QED}$, are obtained by analyzing the corresponding signal MC events as done in data analysis. The cross sections of selected QED processes are calculated with the Babayaga v3.5 generator and the trigger efficiencies are quoted from Ref. [11].

To estimate the numbers of background events, $N^{\rm bkg}_{\rm QED}$, two different methods are applied for $e^+e^- \rightarrow (\gamma)e^+e^-$ and $e^+e^- \rightarrow (\gamma)\gamma\gamma$ processes, individually. For the $e^+e^- \rightarrow (\gamma)e^+e^-$ process, the numbers of background events are estimated by performing the same requirements on the background MC samples, which yields a background level of 10^{-5} after normalization. For $e^+e^- \rightarrow (\gamma)\gamma\gamma$ process, the background level is relatively large due to the hadronic process contamination. The normalized numbers of background events from $e^+e^- \rightarrow (\gamma)\gamma\gamma$ are estimated from the $\Delta\phi_\gamma$ sideband region, defined as $2.5° < |\Delta\phi_\gamma| < 5.0°$. The distributions of the $\Delta\phi_\gamma$ sideband is supposed to be flat by analyzing the background MC samples.

Table 1 shows the input numbers used to calculate the luminosities at $\sqrt{s} = 2.2324$ and 3.0969 GeV.

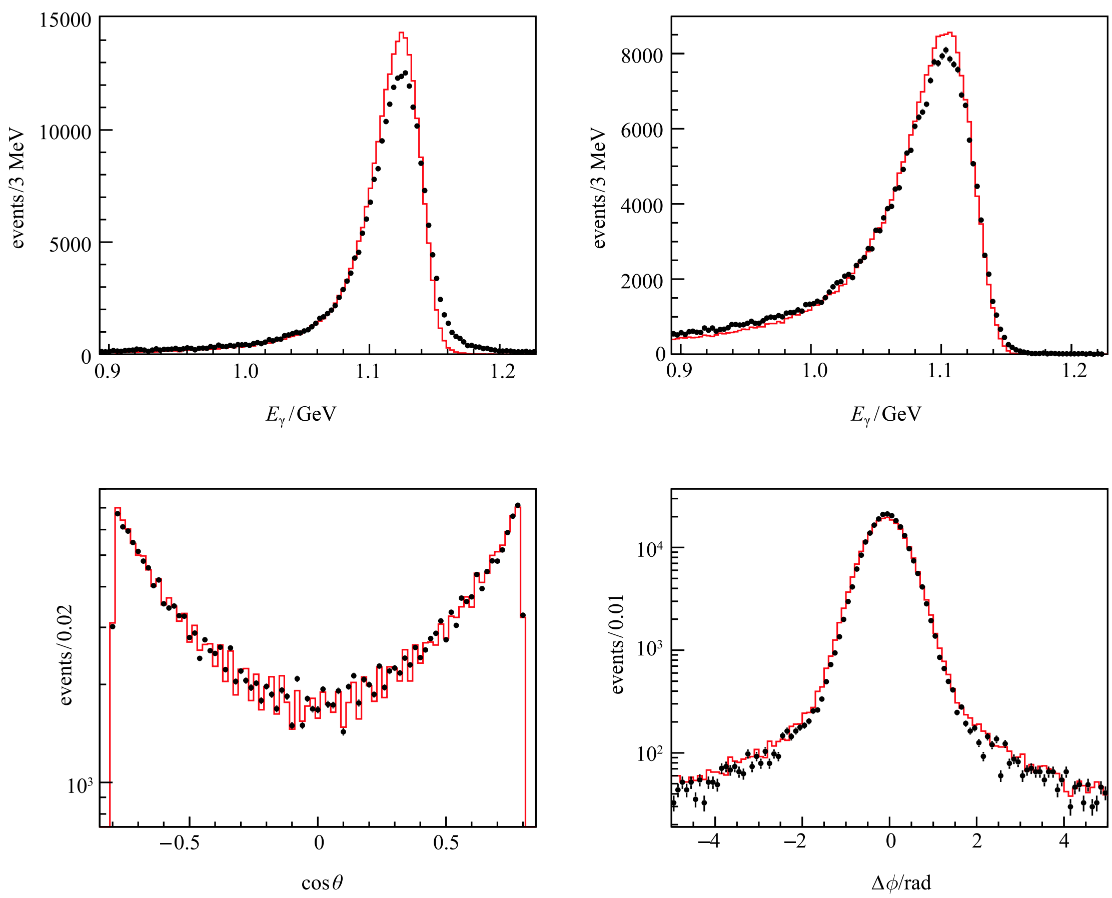

Fig. 2. (color online) Deposited energy distributions of the most energetic γ (upper left), the second most energetic γ (upper right), cosθ (bottom left) and $\Delta\phi$ (bottom right) at $\sqrt{s} = 2.2324$ GeV. Dots with error bars are experimental data and red histograms are signal MC simulation. The MC entries are normalized to the experimental data. The discrepancies in the deposited energy distributions are due to the imperfect simulation of energy correction deposited in the TOF. However, it will not affect the efficiency, since loose requirements on these variables are applied. The uneven distribution of cosθ is due to the structure of the crystals in the EMC.

Table 1. Summaries of the input numbers in luminosity calculation at $\sqrt{s}$ = 2.2324 and 3.0969 GeV.

$\sqrt{s}$/GeV	QED process	$N_{\rm QED}^{\rm obs}$	$N_{\rm QED}^{\rm bkg}$	$\sigma_{\rm QED}$ /nb	$\varepsilon_{\rm QED}(\%)$	$\varepsilon_{\rm QED}^{\rm trig}(\%)$	$\mathcal{L}$/pb^{-1}
2.2324	$(\gamma)e^+e^-$	728522	8	1476.5	18.74	100	2.645
2.2324	$(\gamma)\gamma\gamma$	86974	1138	70.26	46.50	100	2.627
3.0969	$(\gamma)\gamma\gamma$	36083	1062	36.59	46.25	100	2.069

5 Systematic uncertainty

The main systematic uncertainties of the integrated luminosity originate from the uncertainties related to the requirements on the kinematic variables, tracking efficiency, cluster reconstruction efficiency, c.m. energy, MC statistics, background estimation, trigger efficiency and generators.

For the systematic uncertainty from requirements on each kinematic variable, we re-measure the luminosity by altering the required values, i.e., $|\cos\theta| < 0.8$ changes to $|\cos\theta| < 0.75$, $|\Delta\theta_{e^\pm}| < 10°$ changes to $|\Delta\theta_{e^\pm}| < 15°$, $|\Delta\phi_{e^\pm}| < 5°$ changes to $|\Delta\phi_{e^\pm}| < 10°$, $|\Delta\phi_\gamma| < 2.5°$ changes to $|\Delta\phi_\gamma| < 3.0°$, $E_{e^\pm}/E_{\rm beam} > 0.65$ changes to $E_{e^\pm}/E_{\rm beam} > 0.7$ and $0.7 < E_\gamma/E_{\rm beam} < 1.16$ changes to $0.74 < E_\gamma/E_{\rm beam} < 1.2$, individually. The resultant differences of measured luminosity with respect to the nominal value are taken as the systematic uncertainty.

To study the uncertainty of tracking efficiency, a Bhabha event sample is selected with only EMC information [12]. The candidate events are selected by requiring the two clusters detected in the EMC with the deposited energy larger than $0.65 \times E_{\rm beam}$ and having the polar angle $|\cos\theta| < 0.8$, corresponding to the angular coverage of the barrel EMC. The two shower clusters in the xy-plane of the EMC are not back to back, since the two clusters originating from $e^\pm$ in the $e^+e^- \to (\gamma)e^+e^-$ candidate events are bent in the magnetic field. $\Delta\phi_{e^\pm}$ is required to be in the range of $[-40°,-5°]$ or $[5°,40°]$ to remove the $e^+e^- \to (\gamma)\gamma\gamma$ events. We further apply the MDC information on the selected candidates, and the ratio of surviving events is regarded as the tracking efficiency. The average difference in the tracking efficiency between data and signal MC simulation, 0.41%, is taken as the systematic uncertainty.

The systematic uncertainty due to the cluster reconstruction efficiency in the EMC is determined to be 0.05% for $e^\pm$ by comparing the cluster reconstruction efficiencies between data and signal MC (both for e^+ and e^-). Since high-energy γ and $e^\pm$ have similar behaviour in the EMC, the value of 0.05% is also taken as the systematic uncertainty due to the cluster reconstruction efficiency in the EMC for a single γ.

The uncertainty of c.m. energy is estimated to be 2 MeV [13]. For each energy point, an alternative MC simulation sample of 1 million events with a c.m. energy of 2 MeV above the nominal value was generated to re-estimate the detection efficiency, and the difference in the results is regarded as the systematic uncertainty due to c.m. energy.

The uncertainty of MC statistics is 0.17% for the $e^+e^- \to (\gamma)e^+e^-$ process and 0.15% for the $e^+e^- \to (\gamma)\gamma\gamma$ process, which is estimated by

$$\frac{1}{\sqrt{N}} \cdot \sqrt{\frac{(1-\varepsilon)}{\varepsilon}}, \qquad (3)$$

where N is the number of signal MC events, and ε is the detection efficiency.

The rate of background events in the selected $e^+e^- \to (\gamma)e^+e^-$ candidate events is very small (10^{-5}). Therefore, the uncertainty due to background contamination is neglected. For $e^+e^- \to (\gamma)\gamma\gamma$ events, the rate of background events is the normalized number of selected background events in the sideband region divided by the number of signal events, which are $(1.53\pm0.03)\%$ and $(1.31\pm0.04)\%$ for experimental data and the MC simulation, respectively. Therefore, the difference 0.23% is taken as the uncertainty from background contamination.

The trigger efficiencies for barrel $e^+e^- \to (\gamma)e^+e^-$ events and $e^+e^- \to (\gamma)\gamma\gamma$ events are 100% with an uncertainty of less than 0.1% [11].

The uncertainty due to the Babayaga generator v3.5 is 0.5% for $e^+e^- \to (\gamma)e^+e^-$, while 1.0% for $e^+e^- \to (\gamma)\gamma\gamma$ [6].

Table 2. Summary of systematic uncertainties at $\sqrt{s}$ = 2.2324 GeV.

source	$e^+e^- \to (\gamma)e^+e^-$	$e^+e^- \to (\gamma)\gamma\gamma$
$\lvert\cos\theta\rvert < 0.8$	0.12	0.18
$\lvert\Delta\theta_{e^\pm}\rvert < 10°$	0.05	—
$\lvert\Delta\phi_{e^\pm}\rvert < 5°$	0.01	—
$\lvert\Delta\phi_\gamma\rvert < 2.5°$	—	0.07
$E_{e^+}/E_{\rm beam} > 0.65$	0.04	—
$E_{e^-}/E_{\rm beam} > 0.65$	0.05	—
$0.7 < E_\gamma/E_{\rm beam} < 1.16$	—	0.10
tracking efficiency	0.41	—
cluster reconstruction	0.10	0.10
beam energy	0.09	0.09
MC statistics	0.17	0.15
background estimation	0.00	0.23
trigger efficiency	0.10	0.10
generator	0.50	1.00
total	0.70	1.10

Systematic uncertainties at $\sqrt{s}$ = 2.2324 GeV for $e^+e^- \to (\gamma)e^+e^-$ and $e^+e^- \to (\gamma)\gamma\gamma$ are listed in Table 2. Assuming all sources of systematic uncertainties are uncorrelated, the total uncertainty is calculated to be 0.7% for $e^+e^- \to (\gamma)e^+e^-$ and 1.1% for $e^+e^- \to (\gamma)\gamma\gamma$ by adding all the contributions in quadrature. The uncertainties related to the tracking efficiency, cluster reconstruction efficiency, trigger efficiency and generators are common between the different c.m. energy points, while others are c.m. energy dependent and are determined for the different c.m. energy points, individually.

6 Summary

By using the QED processes $e^+e^- \to (\gamma)e^+e^-$ and $e^+e^- \to (\gamma)\gamma\gamma$, the integrated luminosities have been measured for 131 data samples with c.m. energy between 2.2324 and 4.5900 GeV. The precision of integrated luminosity is around 0.7% for $e^+e^- \to (\gamma)e^+e^-$, and around 1.1% for $e^+e^- \to (\gamma)\gamma\gamma$. The total luminosity is 1036.3 pb^{-1}, and the luminosities at the individual c.m. energy points are summarized in Table3. The ratios of the measured luminosities from the two process are illustrated in Fig. 3. The ratios are close to 1 within the uncertainties, which indicates the results from the two measurements are consistent with each other. For each energy point out of the J/ψ resonance region, the luminosity measured by $e^+e^- \to (\gamma)e^+e^-$ is more precise and thus is recommended. For energy points around J/ψ (from 3.0930 to 3.1200 GeV), only the luminosities measured by $e^+e^- \to (\gamma)\gamma\gamma$ are obtained. The measured results are important inputs for physics studies, *e.g.*, the R value measurement and J/ψ resonance parameter measurement.

Table 3. The summaries of measured integrated luminosities from the two QED processes. The first uncertainty is statistical and the second is systematic.

$\sqrt{s}$/GeV	$e^+e^- \to (\gamma)e^+e^-/pb^{-1}$	$e^+e^- \to (\gamma)\gamma\gamma/pb^{-1}$
2.2324	2.645±0.006±0.020	2.627±0.009±0.028
2.4000	3.415±0.007±0.024	3.428±0.011±0.040
2.8000	3.753±0.008±0.026	3.766±0.014±0.042
3.0500	14.893±0.030±0.103	14.919±0.029±0.158
3.0600	15.040±0.030±0.131	15.060±0.029±0.158
3.0800	31.019±0.060±0.189	30.942±0.044±0.338
3.0830	4.740±0.011±0.029	4.769±0.017±0.052
3.0900	15.709±0.031±0.099	15.558±0.030±0.162
3.0930	—	14.910±0.030±0.157
3.0943	—	2.143±0.011±0.023
3.0952	—	1.816±0.010±0.019
3.0958	—	2.135±0.011±0.023
3.0969	—	2.069±0.011±0.024
3.0982	—	2.203±0.011±0.023
3.0990	—	0.756±0.007±0.008

Continued

$\sqrt{s}$/GeV	$e^+e^- \to (\gamma)e^+e^-/pb^{-1}$	$e^+e^- \to (\gamma)\gamma\gamma/pb^{-1}$
3.1015	—	1.612±0.010±0.018
3.1055	—	2.106±0.011±0.022
3.1120	—	1.720±0.010±0.019
3.1200	—	1.264±0.009±0.013
3.4000	1.733±0.005±0.014	1.754±0.012±0.020
3.5000	3.633±0.009±0.025	3.643±0.017±0.040
3.5424	8.693±0.019±0.060	8.711±0.027±0.098
3.5538	5.562±0.013±0.034	5.593±0.021±0.059
3.5611	3.847±0.009±0.028	3.894±0.018±0.043
3.6002	9.502±0.020±0.076	9.620±0.028±0.108
3.6500	48.385±0.094±0.300	48.618±0.065±0.538
3.6710	4.628±0.011±0.028	4.603±0.020±0.052
3.8500	7.967±0.018±0.055	7.962±0.028±0.088
3.8900	7.758±0.018±0.054	7.799±0.028±0.087
3.8950	7.567±0.018±0.053	7.626±0.027±0.085
3.9000	7.575±0.018±0.053	7.631±0.027±0.085
3.9050	7.596±0.018±0.053	7.625±0.027±0.085
3.9100	7.240±0.017±0.050	7.267±0.027±0.082
3.9150	7.454±0.018±0.052	7.533±0.027±0.088
3.9200	6.806±0.016±0.048	6.903±0.026±0.076
3.9250	6.694±0.016±0.046	6.763±0.026±0.075
3.9300	6.735±0.016±0.047	6.825±0.026±0.076
3.9350	7.161±0.017±0.051	7.144±0.027±0.079
3.9400	7.228±0.017±0.050	7.256±0.027±0.082
3.9450	7.590±0.018±0.054	7.608±0.028±0.086
3.9500	7.714±0.018±0.055	7.739±0.028±0.086
3.9550	8.124±0.019±0.056	8.141±0.029±0.090
3.9600	8.489±0.020±0.061	8.548±0.029±0.095
3.9650	7.768±0.018±0.054	7.770±0.028±0.086
3.9700	7.321±0.017±0.051	7.368±0.028±0.082
3.9750	8.062±0.019±0.057	8.050±0.029±0.089
3.9800	7.851±0.019±0.059	7.808±0.028±0.087
3.9850	7.969±0.019±0.057	7.992±0.029±0.089
3.9900	8.024±0.019±0.056	8.104±0.029±0.091
3.9950	7.985±0.019±0.057	7.984±0.028±0.084
4.0000	7.732±0.018±0.056	7.805±0.028±0.088
4.0050	7.537±0.018±0.053	7.567±0.028±0.085
4.0100	7.183±0.017±0.050	7.164±0.027±0.079
4.0120	6.907±0.017±0.051	6.951±0.027±0.079
4.0140	6.694±0.016±0.048	6.716±0.027±0.075
4.0160	6.544±0.016±0.045	6.582±0.026±0.074
4.0180	6.968±0.017±0.049	6.996±0.027±0.078
4.0200	6.726±0.016±0.047	6.735±0.027±0.075
4.0250	6.538±0.016±0.047	6.583±0.026±0.073
4.0300	16.451±0.036±0.115	16.526±0.042±0.187
4.0350	6.706±0.016±0.047	6.687±0.027±0.074
4.0400	6.564±0.016±0.046	6.640±0.027±0.073
4.0500	6.567±0.016±0.047	6.620±0.027±0.076
4.0550	6.927±0.017±0.052	6.934±0.027±0.077
4.0600	6.338±0.015±0.045	6.344±0.026±0.071

Continued

$\sqrt{s}$/GeV	$e^+e^- \to (\gamma)e^+e^-$/pb^{-1}	$e^+e^- \to (\gamma)\gamma\gamma$/pb^{-1}
4.0650	7.022±0.017±0.050	6.980±0.027±0.077
4.0700	7.271±0.017±0.052	7.292±0.028±0.079
4.0800	7.721±0.018±0.054	7.686±0.029±0.085
4.0900	7.611±0.018±0.054	7.647±0.029±0.084
4.1000	7.254±0.017±0.051	7.333±0.029±0.085
4.1100	7.146±0.017±0.050	7.219±0.028±0.080
4.1200	7.648±0.018±0.053	7.728±0.028±0.085
4.1300	7.207±0.017±0.051	7.187±0.029±0.079
4.1400	7.268±0.017±0.051	7.296±0.030±0.082
4.1450	7.774±0.019±0.057	7.837±0.029±0.092
4.1500	7.662±0.018±0.053	7.699±0.028±0.087
4.1600	7.954±0.019±0.056	7.982±0.030±0.090
4.1700	18.008±0.039±0.130	18.012±0.045±0.197
4.1800	7.309±0.018±0.051	7.366±0.029±0.082
4.1900	7.560±0.018±0.052	7.571±0.029±0.084
4.1950	7.503±0.018±0.054	7.535±0.029±0.084
4.2000	7.582±0.018±0.053	7.640±0.030±0.084
4.2030	6.815±0.017±0.048	6.838±0.028±0.080
4.2060	7.638±0.018±0.055	7.660±0.030±0.088
4.2100	7.678±0.018±0.054	7.764±0.030±0.089
4.2150	7.768±0.019±0.054	7.780±0.030±0.087
4.2200	7.935±0.019±0.055	7.963±0.030±0.088
4.2250	8.212±0.020±0.061	8.216±0.031±0.092
4.2300	8.193±0.020±0.057	8.249±0.031±0.093
4.2350	8.273±0.020±0.057	8.365±0.031±0.097
4.2400	7.830±0.019±0.054	7.858±0.030±0.087
4.2430	8.571±0.020±0.060	8.550±0.032±0.096
4.2450	8.487±0.020±0.060	8.523±0.032±0.095
4.2480	8.554±0.020±0.059	8.603±0.032±0.096
4.2500	8.596±0.020±0.060	8.599±0.032±0.095
4.2550	8.657±0.020±0.060	8.611±0.032±0.095
4.2600	8.880±0.021±0.063	8.905±0.032±0.099
4.2650	8.629±0.020±0.061	8.639±0.032±0.099

Continued

$\sqrt{s}$/GeV	$e^+e^- \to (\gamma)e^+e^-$/pb^{-1}	$e^+e^- \to (\gamma)\gamma\gamma$/pb^{-1}
4.2700	8.548±0.020±0.060	8.571±0.032±0.096
4.2750	8.567±0.020±0.060	8.571±0.032±0.099
4.2800	8.723±0.021±0.060	8.747±0.032±0.097
4.2850	8.596±0.020±0.059	8.627±0.032±0.097
4.2900	9.010±0.021±0.062	9.068±0.033±0.102
4.3000	8.453±0.020±0.064	8.456±0.031±0.095
4.3100	8.599±0.021±0.063	8.598±0.032±0.100
4.3200	9.342±0.022±0.065	9.336±0.033±0.109
4.3300	8.657±0.021±0.063	8.625±0.031±0.095
4.3400	8.700±0.021±0.061	8.680±0.031±0.097
4.3500	8.542±0.020±0.064	8.521±0.031±0.094
4.3600	8.063±0.019±0.057	8.084±0.031±0.090
4.3700	8.498±0.020±0.061	8.475±0.032±0.095
4.3800	8.158±0.020±0.060	8.189±0.031±0.092
4.3900	7.460±0.018±0.052	7.547±0.030±0.086
4.3950	7.430±0.018±0.052	7.364±0.030±0.083
4.4000	7.178±0.018±0.050	7.095±0.029±0.084
4.4100	6.352±0.016±0.045	6.390±0.028±0.071
4.4200	7.519±0.018±0.054	7.532±0.030±0.085
4.4250	7.436±0.018±0.052	7.443±0.030±0.083
4.4300	6.788±0.017±0.047	6.778±0.029±0.075
4.4400	7.634±0.019±0.053	7.622±0.030±0.087
4.4500	7.677±0.019±0.054	7.746±0.031±0.087
4.4600	8.724±0.021±0.072	8.731±0.033±0.101
4.4800	8.167±0.020±0.062	8.145±0.032±0.093
4.5000	7.997±0.019±0.056	7.954±0.032±0.088
4.5200	8.674±0.021±0.061	8.550±0.033±0.096
4.5400	9.335±0.022±0.077	9.263±0.034±0.102
4.5500	8.765±0.021±0.066	8.719±0.033±0.098
4.5600	8.259±0.020±0.068	8.117±0.032±0.090
4.5700	8.390±0.020±0.062	8.311±0.033±0.093
4.5800	8.545±0.021±0.060	8.491±0.033±0.094
4.5900	8.162±0.020±0.056	8.076±0.032±0.090

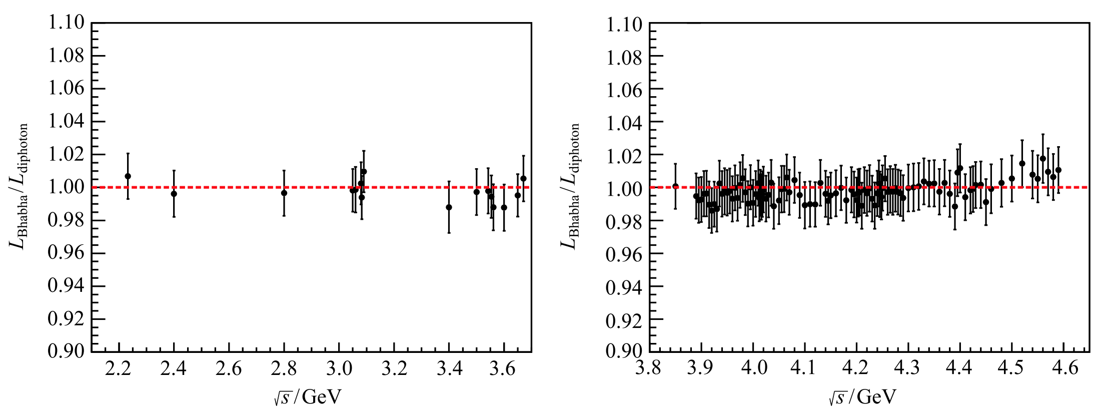

Fig. 3. (color online) The ratios of luminosities measured by $e^+e^- \to (\gamma)e^+e^-$ and $e^+e^- \to (\gamma)\gamma\gamma$. The right-hand plot is for the data samples with c.m. energy larger than 3.8500 GeV, while others are shown in the left-hand plot. The two methods give fully compatible results within the quoted uncertainties.

The BESIII collaboration would like to thank the staff of BEPCII and the IHEP computing center for their dedicated support.

References

1 K. Hagiwara et al, J. Phys. G, **38**: 085003 (2011)
2 M. Davier et al, Eur. Phys. J. C, **71**: 1515 (2011)
3 F. Jegerlehner, arXiv:1511.04473v2 [hep-ph] (2015)
4 M. Ablikim et al (BESIII Collaboration), Nucl. Instrum. Methods A, **614**: 345 (2010)
5 G. Balossini et al, Nucl. Phys. B, **758**: 227 (2006)
6 G. Balossini et al, Phys. Lett. B, **663**: 209 (2008)
7 C. M. Carloni Calame et al, Nucl. Phys. Proc. Suppl., **131**: 48 (2004)
8 S. Jadach, B. F. L. Ward, and Z. Was, Comp. Phys. Commun., **130**: 260 (2000); Phys. Rev. D, **63**: 113009 (2001)
9 B. Andersson, *The Lund Model* (Cambridge University Press, 1998)
10 S. Nova, A. Olchevski, and T. Todorov (DELPHI Collaboration), DELPHI 90-35 PROG, **152** (1990)
11 N.Berger, K. Zhu et al, Chin. Phys. C, **34**: 1779 (2010)
12 M. Ablikim et al (BESIII Collaboration), Chin. Phys. C, **37**: 123001 (2013)
13 M. Ablikim et al (BESIII Collaboration), Chin. Phys. C, **39**: 093001 (2015)